Australia's unique influence on global sea level in 2010–2011

John T. Fasullo,[1] Carmen Boening,[2] Felix W. Landerer,[2] and R. Steven Nerem[3]

Received 3 July 2013; revised 5 August 2013; accepted 5 August 2013; published 27 August 2013.

[1] In 2011, a significant drop in global sea level occurred that was unprecedented in the altimeter era and concurrent with an exceptionally strong La Niña. This analysis examines multiple data sets in exploring the physical basis for the drop's exceptional intensity and persistence. Australia's hydrologic surface mass anomaly is shown to have been a dominant contributor to the 2011 global total, and associated precipitation anomalies were among the highest on record. The persistence of Australia's mass anomaly is attributed to the continent's unique surface hydrology, which includes expansive arheic and endorheic basins that impede runoff to ocean. Based on Australia's key role, attribution of sea level variability is addressed. The modulating influences of the Indian Ocean Dipole and Southern Annular Mode on La Niña teleconnections are found to be key drivers of anomalous precipitation in the continent's interior and the associated surface mass and sea level responses. **Citation:** Fasullo, J. T., C. Boening, F. W. Landerer, and R. S. Nerem (2013), Australia's unique influence on global sea level in 2010–2011, *Geophys. Res. Lett.*, *40*, 4368–4373, doi:10.1002/grl.50834.

1. Introduction

[2] An understanding of variability in global mean sea level (GMSL) as it relates to changes in ocean heat content and terrestrial mass can provide a powerful constraint on the global energy imbalance and terrestrial water cycle variations. Such understanding is also likely to provide useful insight for both monitoring and projecting future sea level changes, which are of considerable socioeconomic importance. While quantifying the steric and mass contributions to GMSL on decadal time scales remains a challenge, the recent availability of surface mass estimates from the Gravity Recovery and Climate Experiment (GRACE) and ocean heat content estimates from the ARGO array of profiling floats provides an unprecedented opportunity to both test closure in the surface mass budget and explore the processes governing GMSL on interannual timescales.

[3] Since 1993, satellite altimetry has provided an estimate of the background rise in sea level of about 3 mm yr^{-1}, while resolving interannual variations of several millimeters. In most years, however, the spread in estimates produced by various data processing centers has not been significantly less than the magnitude of reported interannual variability, posing a major challenge to any quantitative diagnosis [*Masters et al*., 2012]. However, beginning in mid-2010, an anomalous drop in GMSL that was unprecedented in the altimeter era began, reaching a low of about −7 mm in early 2011 and persisting until late that year. Strong agreement on both the magnitude and timing of the drop was reported across processing centers. *Boening et al*. [2012] examined GRACE and ARGO fields during the drop and demonstrated that closure in the surface mass budget was achievable to within the error bounds of ocean heat content estimates. The decrease in GMSL was found to be balanced approximately by an increase in terrestrial mass at low latitudes, attributed to anomalous precipitation over land (P_L). Contributions to the drop arising from steric effects were found to be small (< ~1 mm). Due to established links between ENSO, P_L, and sea level reported in earlier studies [e.g., *Nerem et al*., 2010], the exceptionally strong coincident La Niña was speculated as a likely root cause of the drop.

[4] However, many questions can be raised regarding the drop's broader context within the altimeter era. For instance, why have comparable drops in sea level not been observed during other La Niña events? Do the altimetry and precipitation records suggest a simple relationship between ENSO, P_L, and GMSL, or alternatively, is there an expectation that the relationship may be nonlinear or otherwise complex? Based upon inferences from complementary data, how unique is the 2011 drop in the context of the broader climate record? Finally, given that the timescale of runoff in most river basins is on the order of months, how can a drop in GMSL be sustained for over a year?

[5] To address these questions, we examine multiple observations of the hydrologic cycle. The data and methods used are discussed in section 2, and variability during the GRACE and altimetry records is explored in section 3. In section 4, terrestrial hydrologic anomalies are related to the large-scale evolution of the Tropics and low-frequency modes of variability. We discuss the main results, an examination of the historical record for possible analogues, and implications for both attribution and simulation of the event in models in section 5.

2. Data and Methods

[6] Surface mass variations are estimated from GRACE syntheses created at the Jet Propulsion Laboratory, the University of Texas-Austin, and GFZ Potsdam [*Bettadpur*, 2012; *Watkins and Yuan*, 2012; *Dahle et al*., 2012]. The data provided by these centers are reported on a monthly 1° grid. Due to battery management-related instrument outages starting in 2011, a few GRACE months are either missing or actually partially averaged across 2 months. We interpolate the available GRACE data fields to monthly means and remove climatological monthly means from 2004 to 2010

Additional supporting information may be found in the online version of this article.

[1]National Center for Atmospheric Research, Boulder, Colorado, USA.
[2]Jet Propulsion Laboratory, California Institute of Technology, Pasadena, California, USA.
[3]Colorado Center for Astrodynamics Research, University of Colorado Boulder, Boulder, Colorado, USA.

Corresponding author: J. T. Fasullo, National Center for Atmospheric Research, PO Box 3000, Boulder, CO 80307, USA. (fasullo@ucar.edu)

0094-8276/13/10.1002/grl.50834

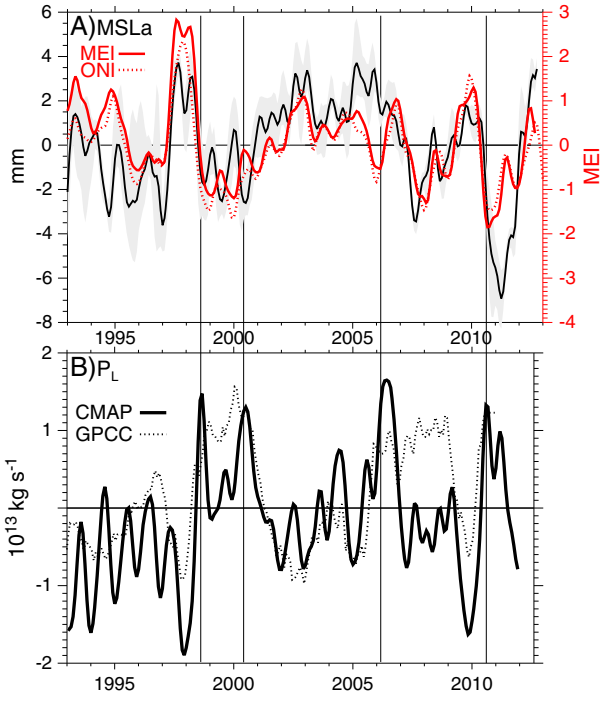

Figure 1. (a) Variations in detrended GMSL are shown for the multi-estimate mean (solid black line) and range (grey shading) and compared to the multivariate ENSO index (MEI, solid red line) and Objective Nino Index (ONI, dotted red line) across the altimeter era with (b) contemporaneous estimates of precipitation over land from CMAP (solid line) and GPCC (dotted line).

to create anomalies. Antarctic surface mass variations are not evaluated though their contribution to global variations on interannual timescales is small [e.g., *Boening et al*., 2012].

[7] Altimetry retrievals of GMSL are based on syntheses of the University of Colorado [*Nerem et al*., 2010], NOAA [*Leuliette et al*., 2004], NASA [*Beckley et al*., 2010], AVISO (Archiving, Validation, and Interpretation of Satellite Oceanographic data) [*Ablain et al*., 2009], and CSIRO (Commonwealth Scientific and Industrial Research Organisation) [*Zhang and Church*, 2012]. Global means are produced by these data centers using various methodologies as discussed in *Masters et al*. [2012]. As uncertainty in GMSL arises both from systematic errors in the retrievals and differences in analysis methodologies, the spread across estimates understates total uncertainty, which therefore remains difficult to quantify [e.g., *Ablain et al*., 2009].

[8] Continental river discharge is estimated from the University of New Hampshire (UNH) Global Runoff Data Center [*Fekete et al*., 2002], while the spatial structure of river basins are taken from Total Runoff Integrating Pathways river basin data set [*Oki and Sud*, 1998].

[9] The Global Precipitation Climatology Centre (GPCC) Version 6 Full Data Reanalysis [*Becker et al*., 2013] is used to assess global land precipitation. It benefits from a greater density of input gauge observations and fewer unmonitored areas in comparison to other gauge data sets and extends from 1901 to 2010. Over Australia, we also use the Australian Water Availability Project (AWAP) gauge synthesis of *Jones et al*. [2009]. Global precipitation retrievals from Climate Prediction Center Merged Analysis of Precipitation (CMAP) [*Xie and Arkin*, 1996] are also used to estimate global land and ocean conditions based on their monthly 2.5° gridded product. Quarter-degree retrievals from TRMM's 3B43 product are also used [*Liu et al*., 2012]. Atmospheric moisture transports are diagnosed from ERA Interim vertically integrated budgets described in *Trenberth et al*. [2011].

3. Variability Across the Altimetry and GRACE Records

[10] To explore the hypothesis that the 2011 GMSL drop owed its intensity to La Niña, we summarize the evolution of GMSL, ENSO, and P_L in Figure 1. ENSO is estimated from both the Multivariate ENSO Index [*Wolter and Timlin*, 1998] and the Objective Niño Index (ONI), while GMSL is estimated from the mean and range of altimeter estimates, and P_L is estimated from both CMAP and GPCC. While ENSO indices correlate positively with GMSL across the altimeter record (Figure 1a, $r = 0.40$ to 0.58 for the various altimeter data sets), the multivariate ENSO Index (MEI) explains only about a quarter of its variance when fit to the sea level record. Also notable is the inability of either the MEI or ONI to explain a majority of the GMSL drop in 2011, even when scaled to overestimate the magnitude of other major El Niño events (e.g., 1998 and 2010). In addition, when P_L is correlated against the time derivative of GMSL (not shown), the relationship is exceptionally weak ($-0.2 > r > -0.3$). Moreover, the P_L anomaly in 2011 is not exceptional and is comparable to several other intervals in the altimeter record (e.g., 2000 and 2006) during which time GMSL drops are altogether absent. Strong linkages between P_L and GMSL are similarly absent when judged using other precipitation products (e.g., GPCP) and reanalysis atmospheric budgets (not shown). This thus begs the question that given the unexceptional nature of the 2010–2011 P_L anomaly, why was the magnitude and persistence of the drop in GMSL so large? It is therefore suggested that the state of ENSO, by itself, is not a strong determinant of the root processes that govern GMSL and that other factors are therefore essential. Support for this perspective is developed in greater depth in the following sections.

[11] The evolution of GRACE surface mass retrievals for the continents contributing to the 2011 mass increase is summarized in Figure 2. Also shown are ratios of river discharge to precipitation (RR), based on the UNH river discharge dataset, and the percentage contribution to the net change in mass from mid-2010 to mid-2011 based on the GRACE estimates' mean (ΔM). Continents with a low RR have a longer residence time of precipitated water since runoff is small. Continents with small net changes in mass between 2010 and 2011 include Eurasia (−0.5%) and Africa (−13%), which are therefore not shown.

[12] The 2011 GMSL drop began in early 2010 (Figure 1), coincident with a mean negative anomaly in global land mass of $-5.2 \cdot 10^{14}$ kg (Figure 2, top panel) at a time of strong agreement among the various GRACE estimates. As the drop intensified, the terrestrial mass anomaly also increased, peaking in mid-2011 at about $1.39 \cdot 10^{15}$ kg. By late 2011, about 18 months after its onset, the global mean mass anomaly had largely dissipated.

[13] In both Australia and South America, significant mass deficits precede the onset of the GMSL drop and emerge in early 2009 and 2010, respectively, concurrent with the onset and peak of the 2010 El Niño. The initial increase in mass in

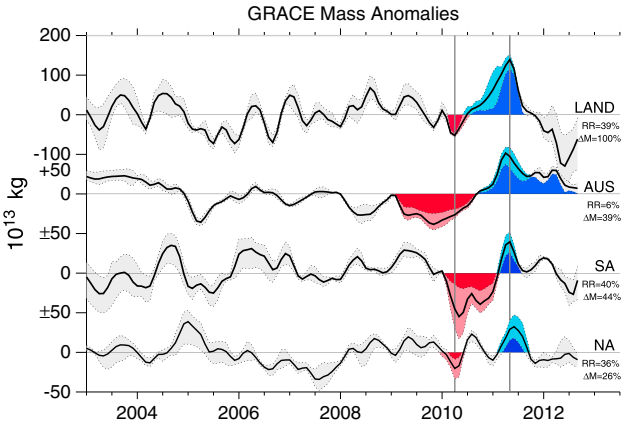

Figure 2. The evolution of detrended GRACE land mass anomalies is shown for the globe and for continents with substantial contribution to the 2011 global mass increase including Australia (AUS), South America (SA), and North America (NA). The multi-estimate range is shaded. The 2010 minimum and 2011 maximum are highlighted, as are related deficits (red) and excesses (blue). Also shown are the runoff ratio (RR) and contribution to the global change from the 2010 minimum to the 2011 peak. Time series are smoothed with a 1-2-1 smoother. For reference, a 5 mm GMSL rise is equivalent to roughly $1.85 \cdot 10^{15}$ kg.

these regions during the 2011 drop thus actually represents a recovery from drought and contributes significantly to the increase in mass from 2010 to 2011. By early 2011, mean mass anomalies for both continents had become positive, growing substantially into mid-2011 and comprising the dominant contributors to the global land anomaly. Large contrasts in precipitation between El Niño and La Niña in South America are characteristic of ENSO's influence generally (Figure S1 in the supporting information), while as discussed below, variability in Australia was exceptional. It is noteworthy that the disagreement among estimates of the mass anomaly in mid-2010 in South America is comparatively large and undermines precise quantitative statements regarding its broader role in changes between 2010 and 2011.

[14] More consistently depicted among GRACE estimates are the relative magnitude and persistence of positive mass anomalies and their contrast between the continents. In Australia, positive anomalies are exceptionally persistent and intense through 2011, even when area integrated as in Figure 2. In fact, through the end of the available data record (late 2012), the positive mass anomaly persists for Australia while dissipating for land generally and all other continents contributing to the original global anomaly. The unique persistence of Australian mass is also evident across the length of the GRACE record, as Australia has greater power in mass at low frequencies than any other continent (Figure S2). These findings agree qualitatively with expectations based on the exceptionally low runoff ratio of Australia (6%) relative to other continents (~40%), the expansive nature of its arheic and endorheic drainage basins [e.g., *Tweed et al.*, 2011], and the longer timescale therefore associated with dissipation of surface mass anomalies.

[15] Lastly, while variability in North America contributes to an increase in global mass across the GMSL drop, anomalies vary considerably during the drop itself before peaking in mid-2011. Compositing GPCC precipitation across multiple ENSO events in the twentieth century (not shown) suggests that North American variability during 2011 is not characteristic generally of La Niña and may be the result of stochastic variability rather than being a response to tropical forcing. If so, the contribution from North America may be most appropriately viewed as a serendipitous amplification of the 2011 GMSL drop rather than a canonical result of La Niña's teleconnections. Further consideration in resolving this point remains warranted and is not the main subject of this work.

4. Tropical Mass Anomalies in the Context of Major Tropical Modes

[16] The GRACE record provides an unprecedented opportunity to assess variations in the surface mass budget on a global scale. When interpreted in conjunction with precipitation, it can also assist in the interpretation of interactions between surface mass and large-scale modes of variability. Given their importance in the global budget, mass anomalies in Australia and South America are examined here as they relate to the dominant large-scale modes influencing precipitation in these regions, including ENSO (i.e., MEI), Indian Ocean Dipole (IOD), and Southern Annular Mode (SAM) [e.g., *Risbey et al.*, 2009]. Figure 3 summarizes the evolution of surface mass and precipitation as these modes evolve from early 2010 through late 2011, where 6 month averages are shown in order to reduce noise inherent to GRACE retrievals [e.g., *Trenberth and Fasullo*, 2013] and resolve large-scale structures. Precipitation averages are offset 3 months from mass averages in order to assist in inferring their relationship to mass tendencies. Atmospheric moisture transports, precipitation, and storage for Australia provide additional context for interpreting the large-scale variability shown in Figure 3 and are assessed in Figure 4.

[17] Prior to the event (January–June 2010), surface mass anomalies are negative over western Australia and north-central South America and contribute significantly to the continent-wide deficits reported in Figure 2. From March through August 2010, a strong positive SAM is established while La Niña and a negative IOD anomaly are rapidly transitioning to their largest values during the altimeter era (Figure 4c). Combined with the long-term trend in SST, these modes contribute to a strong warm anomaly in the equatorial eastern Indian and western Pacific Oceans [*Hendon et al.*, 2013]. From July–October 2010, large anomalous northerly moisture transport emanates from the Tropics and flows northwesterly over central and eastern Australia (Figure 4a). There is strong spatial coherence between this anomalous transport and precipitation anomalies that is suggestive of a direct physical linkage, consistent with *Hendon et al.* [2013] who find the mutual interaction of the SAM, a strong La Niña, and anomalously warm sea surface temperatures north of Australia to play a central role in the exceptional Australian precipitation during this period. The persistent, continental-scale nature of precipitation anomalies in late 2010 (Figure 4a) stands in contrast to the regionally and seasonally varying structures that typically accompany La Niña or SAM teleconnections. In South America, as the La Niña has yet to reach its peak, only sporadic positive precipitation anomalies are evident, with negative anomalies persisting over much of central South America.

[18] In subsequent mass anomalies (July–December 2010), the influences of March–August precipitation anomalies are

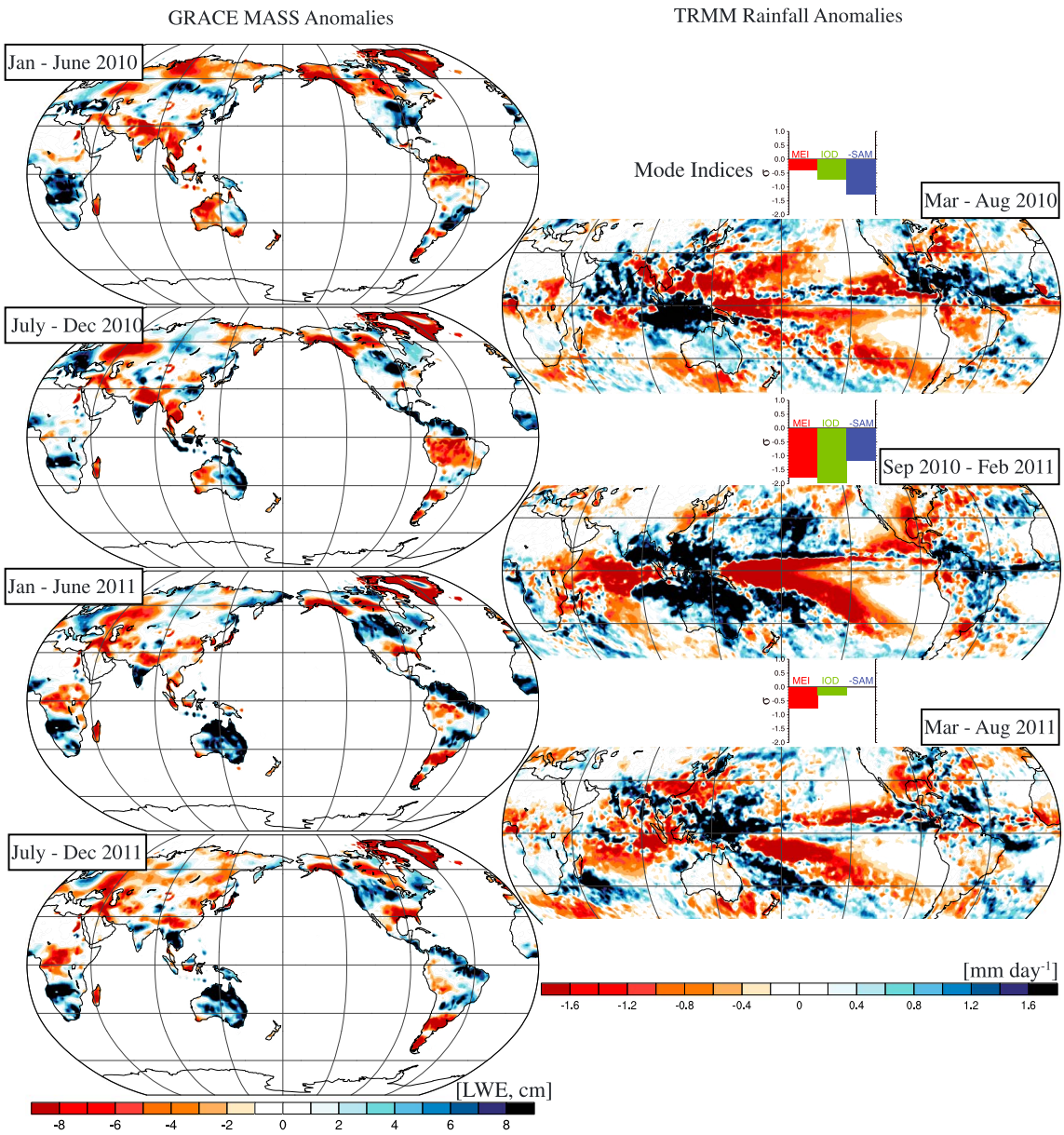

Figure 3. Evolution of GRACE (left column) and TRMM anomalies (right column) for 6 month intervals during 2010 and 2011. Intervals shown for TRMM anomalies are offset by 3 months in order to provide context for changes in mass. Also shown are indices of the major modes influencing Australia: the MEI, IOD, and SAM.

evident. Negative mass anomalies in western Australia and north South America weaken and shrink, while in central South America, they intensify in regions where precipitation anomalies from January to June were negative, contributing to the continent-wide negative mass anomaly (Figure 2). As the La Niña and IOD events mature in late 2010 into early 2011, their signature in tropical precipitation becomes clearer. Strong zonal gradients in both the Pacific and Indian Ocean reflect established La Niña and negative IOD conditions, respectively. Together, these are associated with exceptional low-level convergence in the eastern Indian and western Pacific Oceans and associated northerly transport of moisture across northern Australia associated with both westerlies emanating from the Indian Ocean and easterlies originating in the Pacific (Figure 4a, right panel) that supply moisture to associated precipitation anomalies spanning much of inland Australia. In South America, positive precipitation anomalies similar in magnitude to other recent major La Niña events are evident (e.g., Figure S1).

[19] By January–June 2011, mass anomalies are strongly positive in both Australia and South America (Figure 2) reflecting a major net increase in surface water by these continents. Other continents (e.g., Africa, Eurasia, and North America) are characterized by large regional surface mass anomalies, but generally, these compensate each other and limit their net contribution to the global total. Averaged from March through August 2011, IOD and SAM anomalies are near zero and only a weak La Niña persists (also Figure 4c). Mean precipitation anomalies in Australia and South America are unremarkable generally relative to earlier intervals. Following this period (July–December 2011), both positive and negative mass anomalies weaken considerably in South America with negative anomalies in the west balancing approximately positive anomalies along the northern coast and south of

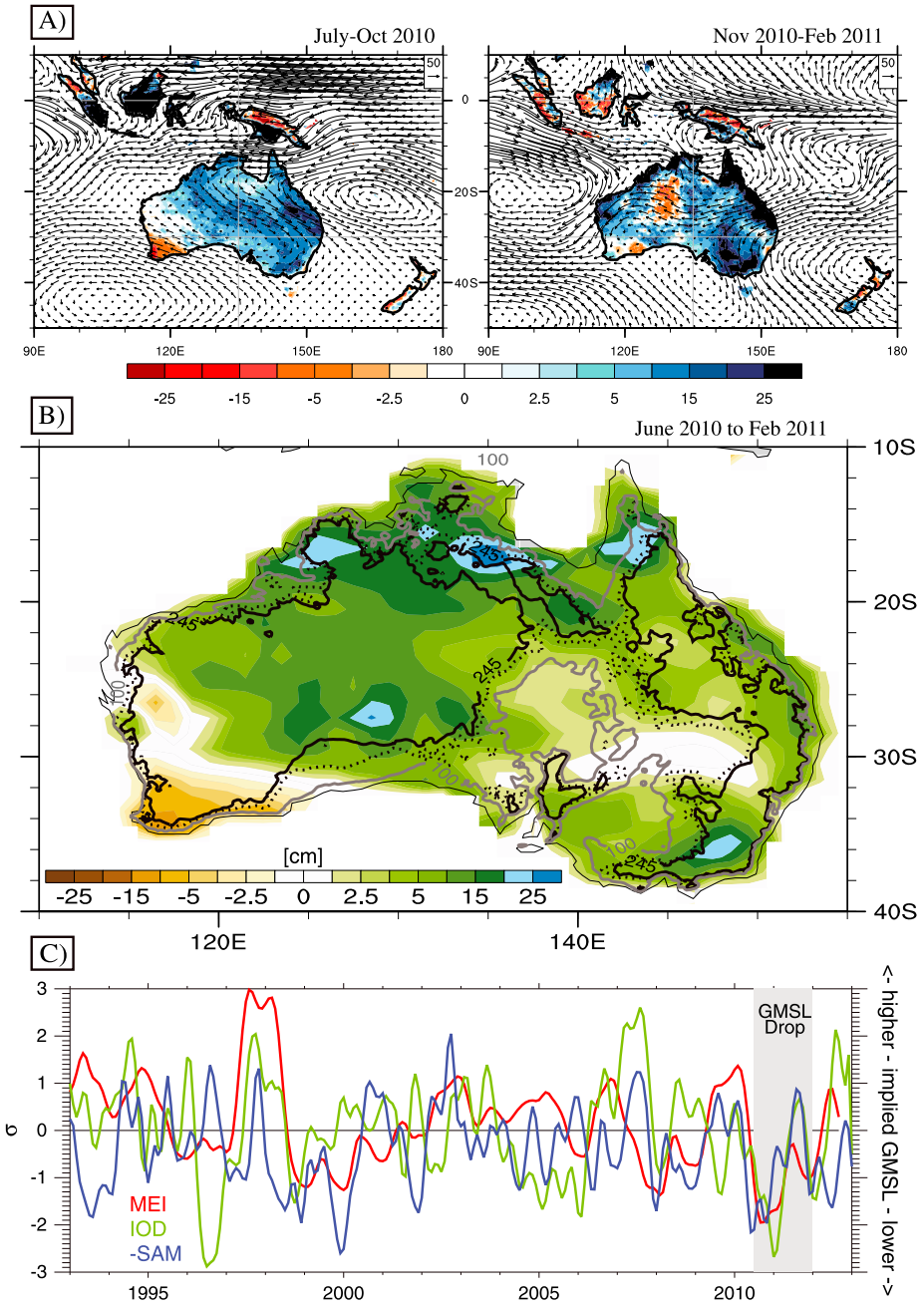

Figure 4. (a) Anomalies in TRMM precipitation (colors, 0.1 mm day^{-1}) and ERA-I water vapor transport (vectors, kg m^{-1} s^{-1}) during the months of peak SAM (left) and MEI/IOD (right). (b) The change in mass in Australia as reported by GRACE-CSR from June 2010 to Feb 2011. Contours represent land surface elevation isopleths (0 m, 100 m, 190 m, and 245 m) in order to emphasize the Western Plateau (west) and saddle point in northeast Australia, south of which rivers flow into the continent's interior. (c) Evolution of major modes influencing Australian precipitation.

the Amazon to result in a small mean anomaly (Figure 2). Over Australia, strong mass anomalies persist, resembling those in January–June 2011 in both spatial structure and magnitude. Across much of the continent, these persist well into 2012.

5. Discussion and Conclusion

[20] Interannual variations in continental water storage can have a profound influence on GMSL that in some years overwhelm the background trend. Here it is shown that Australia contributes uniquely and substantially to the intensity and persistence of the global land hydrologic mass increase during the 2011 sea level drop. South America, while showing a considerable, though quantitatively less certain, increase in mass from 2010 to 2011, exhibits only a transient positive mass anomaly in 2011. The brevity of the anomaly is qualitatively consistent with its surface hydrology, which in most regions such as the Amazon is well conditioned for river runoff and discharge to ocean. In contrast, the persistence of Australian mass anomalies is consistent with the impediment to runoff posed by its arheic and endorheic basins.

[21] The unique contribution of Australia to global mass anomalies provides the opportunity to reframe attribution of GMSL variability in terms of the root drivers of Australian precipitation and draw upon the insights of recent work. The findings of *Risbey et al*. [2009] and *Hendon et al*. [2013] highlight the roles of the IOD and SAM in driving low-frequency variability in La Niña's teleconnections. Here, we find these to likely be key influences on terrestrial hydrologic processes influencing the 2011 GMSL drop. Combined with a consideration of Australia's surface hydrology, which contributes to a runoff ratio of only 6%, a physical basis is thus provided for the complex and variable nature of ENSO's relationship to GMSL in recent years. These modes also provide a broader perspective on the altimeter record and the uniqueness of the 2011 GMSL drop, as this represents the first La Niña in the altimeter era to coincide with strong and sustained negative IOD and positive SAM anomalies. The gauge record of precipitation further supports this interpretation by demonstrating that the periods of strongest precipitation in Australia's arheic and endorheic basins do not generally coincide with the strongest La Niña events (e.g., 1955/6, also Figure S4), but with intervals in which the IOD and SAM are conducive to the intrusion of tropical moisture transports to the continent's interior (e.g., 1973/4).

[22] Implications for modeling the 2011 GMSL drop are considerable as these findings highlight the importance of continental interior basins, which in climate models are generally not realistically simulated. In these regions, most models implement an unphysical discharge of accumulated water to the ocean such that the basins do not themselves accumulate mass, irrespective of the intensity of precipitation and runoff. This limits the ability of models to simulate the surface mass anomaly and associated sea level deficit and undermines comparison and evaluation with GRACE data.

[23] Lastly, the current global sea level anomaly is an interesting counterpoint to the 2011 drop, with strongly positive anomalies in mid-2013 accompanying ENSO neutral conditions. The event appears to further emphasize the need to understand deviations of GMSL independent of ENSO. Given the results of this work, a plausible working hypothesis to be explored further relates to the role of Australia's exceptional heat wave and drought of early 2013 in the global surface mass budget. In conjunction with the major prevailing droughts in the Americas [*Hoerling et al*., 2012], these anomalies are promising candidates to be involved in the 2013 peak and deserve scrutiny in GRACE surface mass estimates as they become available. Better understanding such variability is likely to be fundamental in interpreting low-frequency variability and trends in the growing altimetry and surface mass data records.

[24] **Acknowledgments.** John T. Fasullo's participation in this work is supported by NASA awards NNG06GB91G and NNH11ZDA001N and NSF award NSF-AGS-1243107. The National Center for Atmospheric Research (NCAR) is sponsored by the National Science Foundation. Part of the research was carried out at the Jet Propulsion Laboratory, California Institute of Technology under a contract with the National Aeronautics and Space Administration.

[25] The Editor thanks Matthew Wheeler and Don Chambers for their assistance in evaluating this paper.

References

Ablain, M., A. Cazenave, S. Guinehut, and G. Valladeau (2009), A new assessment of global mean sea level from altimeters highlights a reduction of global slope from 2005 to 2008 in agreement with in-situ measurements, *Ocean Sci.*, *5*(2), 193–201.

Becker, A., P. Finger, A. Meyer-Christoffer, B. Rudolf, K. Schamm, U. Schneider, and M. Ziese (2013), A description of the global land-surface precipitation data products of the Global Precipitation Climatology Centre with sample applications including centennial (trend) analysis from 1901–present, *Earth Syst. Sci. Data*, *5*, 71–99, doi:10.5194/essd-5-71-2013.

Beckley, B. D., N. P. Zelensky, S. A. Holmes, F. G. Lemoine, R. D. Ray, G. T. Mitchum, S. Desai, and S. T. Brown (2010), Assessment of the Jason-2 extension to the TOPEX/Poseidon, Jason-1 sea-surface height time series for global mean sea level monitoring, *Marine Geodesy*, *33*(S1), 447–471, Supplemental Issue on OSTM/Jason-2 calibration/validation, Vol. 1, doi:10.1080/01490419.2010.491029.

Bettadpur, S. (2012), UTCSR Level-2 Processing Standards Document for Level-2 Product Release 0005, (Scientific Technical Report - Data, 12/05), Austin, 16 p. [Available at ftp://podaac.jpl.nasa.gov/allData/grace/docs/L2-CSR0005_ProcStd_v4.0.pdf.]

Boening, C., J. K. Willis, F. W. Landerer, R. S. Nerem, and J. Fasullo (2012), The 2011 La Niña: So strong, the oceans fell, *Geophys. Res. Lett.*, *39*, L19602, doi:10.1029/2012GL053055.

Dahle, C., et al. (2012), GFZ GRACE Level-2 Processing Standards Document for Level-2 Product Release 0005, (Scientific Technical Report - Data , 12/02), Potsdam, 20 p., doi:10.2312/GFZ.b103-12020.

Fekete, B. M., C. J. Vörösmarty, and W. Grabs (2002), High-resolution fields of global runoff combining observed river discharge and simulated water balances, *Global Biogeochem. Cycles*, *16*(3), 1042, doi:10.1029/1999GB001254.

Hendon, H. H., E. P. Lim, J. M. Arblaster, and D. L. Anderson (2013), Causes and predictability of the record wet east Australian spring 2010, *Clim. Dyn.*, 1–20. [available at http://link.springer.com/content/pdf/10.1007%2Fs00382-013-1700-5.pdf.]

Hoerling, M., A. Kumar, R. Dole, J. W. Nielsen-Gammon, J. Eischeid, J. Perlwitz, and M. Chen (2012), Anatomy of an extreme event, *J. Climate*, *26*, 2811–2832, doi:10.1175/JCLI-D-12-00270.1.

Jones, D. A., W. Wang, and R. Fawcett (2009), High-quality spatial climate data-sets for Australia, *Aust Meteorol Oceanogr J*, *58*, 233–248.

Leuliette, E. W., R. S. Nerem, and G. T. Mitchum (2004), Calibration of TOPEX/Poseidon and Jason altimeter data to construct a continuous record of mean sea level change, *Mar. Geod.*, *27*(1–2), 79–94, doi:10.1080/01490410490465193.

Liu, Z., D. Ostrenga, W. Teng, S. Kempler, and M. Greene (2012), TRMM precipitation application examples using data services at NASA GES DISC.

Masters, D., R. S. Nerem, C. Choe, E. Leuliette, B. Beckley, N. White, and M. Ablain (2012), Comparison of global mean sea level time series from TOPEX/Poseidon, Jason-1, and Jason-2. *Mar. Geod.*, *35*(sup1), 20–41.

Nerem, R. S., D. P. Chambers, C. Choe, and G. T. Mitchum (2010), Estimating mean sea level change from the TOPEX and Jason altimeter missions, *Mar. Geod.*, *33*, 435–446, doi:10.1080/01490419.2010.491031.

Oki, T., and Y. C. Sud (1998), Design of Total Runoff Integrating Pathways (TRIP)—A global river channel network, *Earth Interactions*, *2*.

Risbey, J. S., M. J. Pook, P. C. McIntosh, M. C. Wheeler, and H. H. Hendon (2009), On the remote drivers of rainfall variability in Australia, *Monthly Weather Review*, *137*(10), 3233–3253, doi:10.1175/2009MWR2861.1.

Trenberth, K. E., and J. T. Fasullo (2013), North American water and energy cycles, *Geophys. Res. Lett.*, *40*, 365–369, doi:10.1002/grl.50107.

Trenberth, K. E., J. T. Fasullo, and J. Mackaro (2011), Atmospheric moisture transports from ocean to land and global energy flows in reanalyses, *J. Climate*, *24*, 4907–4924, doi:10.1175/2011JCLI4171.1.

Tweed, S., M. Leblanc, I. Cartwright, G. Favreau, and C. Leduc (2011), Arid zone groundwater recharge and salinisation processes; An example from the Lake Eyre Basin, Australia, *J. Hydrology*, *408*(3), 257–275.

Watkins, M. M., and D.-N. Yuan (2012), JPL Level-2 Processing Standards Document For Level-2 Product Release 05, (Scientific Technical Report - Data , 12/03), Pasadena, 14 p. [Available at ftp://podaac.jpl.nasa.gov/allData/grace/docs/L2-JPL_ProcStds_v5.pdf.]

Wolter, K., and M. S. Timlin (1998), Measuring the strength of ENSO events: How does 1997/98 rank?, *Weather*, *53*, 315–324.

Xie, P., and P. A. Arkin (1996), Analysis of global monthly precipitation using gauge observations, satellite estimates, and numerical model predictions, *J. Clim.*, *9*, 840–858.

Zhang, X., and J. A. Church (2012), Sea level trends, interannual and decadal variability in the Pacific Ocean, *Geophys. Res. Lett.*, *39*, L21701, doi:10.1029/2012GL053240.